Title

Adduction-Induced Strain on the Optic Nerve in Primary Open Angle Glaucoma at Normal Intraocular Pressure.

Journal

Current eye research, 46(4)

ISSN

0271-3683

Authors

Clark, Robert A
Suh, Soh Youn
Caprioli, Joseph
et al.

Publication Date

2021-04-01

DOI

10.1080/02713683.2020.1817491

Peer reviewed

Current Eye Research

ISSN: (Print) (Online) Journal homepage: https://www.tandfonline.com/loi/icey20

Adduction-Induced Strain on the Optic Nerve in Primary Open Angle Glaucoma at Normal Intraocular Pressure

Robert A. Clark, Soh Youn Suh, Joseph Caprioli, JoAnn A. Giaconi, Kouros Nouri-Mahdavi, Simon K. Law, Laura Bonelli, Anne L. Coleman & Joseph L. Demer

To cite this article: Robert A. Clark, Soh Youn Suh, Joseph Caprioli, JoAnn A. Giaconi, Kouros Nouri-Mahdavi, Simon K. Law, Laura Bonelli, Anne L. Coleman & Joseph L. Demer (2021) Adduction-Induced Strain on the Optic Nerve in Primary Open Angle Glaucoma at Normal Intraocular Pressure, Current Eye Research, 46:4, 568-578, DOI: 10.1080/02713683.2020.1817491

To link to this article: https://doi.org/10.1080/02713683.2020.1817491

Published online: 11 Sep 2020.

CURRENT EYE RESEARCH
2021, VOL. 46, NO. 4, 568–578
https://doi.org/10.1080/02713683.2020.1817491

Taylor & Francis
Taylor & Francis Group

Adduction-Induced Strain on the Optic Nerve in Primary Open Angle Glaucoma at Normal Intraocular Pressure

Robert A. Clark[a,b], Soh Youn Suh[a,b], Joseph Caprioli[a,b], JoAnn A. Giaconi[a,b], Kouros Nouri-Mahdavi[a,b], Simon K. Law[a,b], Laura Bonelli[a,b], Anne L. Coleman[a,b,c], and Joseph L. Demer[a,b,d,e,f]

[a]Department of Ophthalmology, University of California, Los Angeles, USA; [b]Stein Eye Institute, University of California, Los Angeles, USA; [c]Department of Epidemiology Fielding School of Public Health, University of California, Los Angeles, USA; [d]Department of Neurology, University of California, Los Angeles, USA; [e]Neuroscience Interdepartmental Program, University of California, Los Angeles, USA; [f]Bioengineering Interdepartmental Program, University of California, Los Angeles, USA

ABSTRACT

Purpose/Aim: The optic nerve (ON) becomes taut during adduction beyond ~26° in healthy people and patients with primary open angle glaucoma (POAG), but only retracts the globe in POAG. We used magnetic resonance imaging (MRI) to investigate this difference.

Materials and Methods: MRI was obtained in 2-mm quasi-coronal planes in central gaze, and smaller (~23-25°) and larger (~30-31°) adduction and abduction in 21 controls and 12 POAG subjects whose intraocular pressure never exceeded 21 mmHg. ON cross-sections were analyzed from the globe to 10 mm posteriorly. Area centroids were used to calculate ON path lengths and changes in cross-sections to calculate elongation assuming volume conservation.

Results: For both groups, ON path was nearly straight (<102.5% of minimum path) in smaller adduction, with minimal further straightening in larger adduction. ON length was redundant in abduction, exceeding 103% of minimum path for both groups. For normals, the ON elongated 0.4 ± 0.5 mm from central gaze to smaller adduction, and 0.4 ± 0.5 mm further from smaller to larger adduction. For POAG subjects, the ON did not elongate on average from central gaze to smaller adduction and only 0.2 ± 0.4 mm from smaller to larger adduction (P = .045 vs normals). Both groups demonstrated minimal ON elongation not exceeding 0.25 mm from central gaze to smaller and larger abduction. The globe retracted significantly more during large adduction in POAG subjects than normals (0.6 ± 0.7 mm vs 0.2 ± 0.5 mm, P = .027), without appreciable retraction in abduction. For each mm increase in globe axial length, ON elongation in large adduction similarly increased by 0.2 mm in each group.

Conclusions: The normal ON stretches to absorb force and avert globe retraction in adduction. In POAG with mild to severe visual field loss, the relatively inelastic ON tethers and retracts the globe during adduction beyond ~26°, transfering stress to the optic disc that could contribute to progressive neuropathy during repeated eye movements.

ARTICLE HISTORY
Received 28 July 2020
Revised 12 August 2020
Accepted 19 August 2020

KEYWORDS
Biomechanics; normal tension glaucoma; optic nerve; optic nerve strain

Introduction

The physiologic range of eye movements has been classically considered to be limited only by orbital check ligaments.[1] Recently, it was recognized that the optic nerve (ON) can also check eye rotation, restricting adduction.[2–5] Orbital magnetic resonance imaging (MRI) in adduction demonstrates that ON path redundancy, the difference between actual ON length and the minimum straight-line length between orbital apex and globe, is typically exhausted when adduction exceeds about 26° (Figure 1),[2–4] an angle much smaller than the roughly 40° normal physiological adduction limit.[6] We have elsewhere summarized evidence that large eye movements are common in daily life.[3,5,7] Once the limit of relaxed ON length has been reached, further adduction necessarily requires that the ON stretch, or that globe position be displaced, or both. Regardless of the combination, ON tethering in adduction imposes tensile (i.e. stretching) mechanical force on the ON and its sheath[4] sufficient to produce deformation of the ON head measurable by scanning laser ophthalmoscopy[8] and optical coherence tomography.[9]

The rationale for the current study, and its relationship to primary open angle glaucoma (POAG), requires context of some biomechanical definitions. Tensile force applied to any material produces elongation; in biomechanics, this elongation is termed "strain." A given tensile force applied to a highly elastic, soft material produces a larger strain (relative elongation, often expressed in percent of original length) than that force applied to a stiffer, less elastic material that consequently experiences less strain. Conversely, less tensile force is required for a given elongation applied to the highly elastic, soft material, while greater tensile force is required when applied to the stiffer, less elastic material. In biomechanics, "stress" is defined as force divided by the cross-sectional area of the piece of material acted upon. Stress has the same units as hydrostatic pressure. For example, the common intraocular pressure (IOP) unit of 1 mmHg is the equivalent of 133 Pascal, a metric unit defined as 1 Newton

CONTACT Joseph L. Demer jld@jsei.ucla.edu Stein Eye Institute, Los Angeles, CA 90095-7002

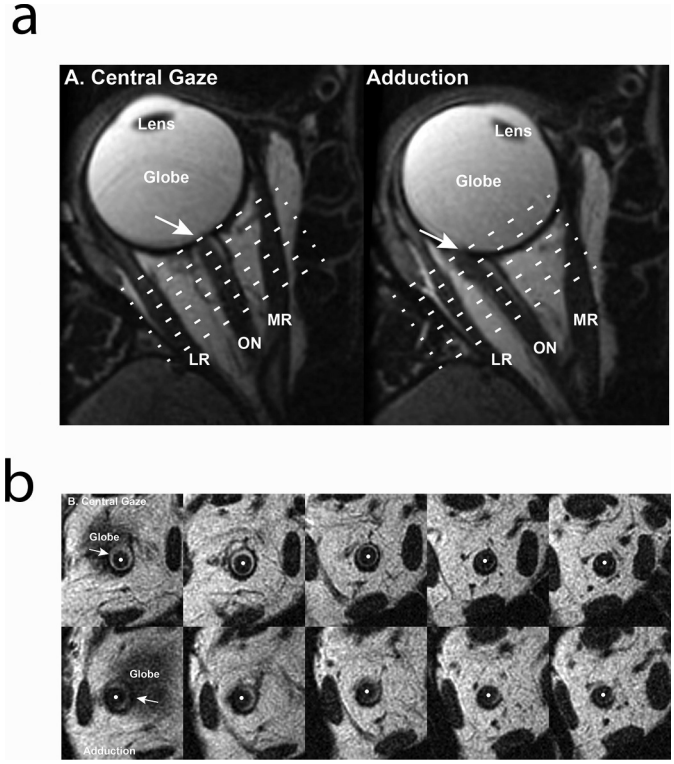

Figure 1. MRI in normal subject. **a**. In central gaze (left), this optic nerve (ON) already exhibited minimal redundancy. During adduction (right), the posterior globe rotated laterally. Quasi-coronal magnetic resonance imaging was in planes perpendicular to the long axis of the orbit (dashed white lines). Optic nerve (ON) cross-sections were analyzed in the five image planes posterior to the globe-ON junction (white arrows). **b**. For these five 2-mm thick image planes arranged from anterior to posterior beginning at the globe at left, the optic nerve (white dots) and inner border of its sheath were outlined. Note that the optic nerve cross-section is smaller and more temporally eccentric within its sheath during adduction (bottom) than in central gaze (top).

(kg-m/s^2) force per square meter. Thus, IOP is a stress applied to the ON from inside the eye, while adduction applies a physically identical type of stress to the ON, but from outside the eye.

Analysis of the response of the globe and ON to this mechanical force during adduction tethering is complicated by the fact that the globe does not simply rotate about its center.[10,11] Instead, eye movements combine globe rotation and globe translation around an eccentric rotational axis.[10,11] For example, as the medial rectus (MR) muscle contracts, the globe normally both rotates into adduction and translates medially almost one mm.[10,11] The globe's dynamic behavior, however, differs in patients who have POAG.[3,5] In particular, MRI performed in patients who have POAG with[5] or without[3] elevated IOP (above the population statistical normal upper limit of 21 mmHg) demonstrates that the globe retracts by almost one mm during adduction, a phenomenon neither observed in abduction nor in the normal population during either adduction or abduction.[3,5] When IOP in a patient with POAG has never been measured to exceed the normal range, this subset of POAG is termed by some to represent "normal-tension glaucoma (NTG)." In some populations, NTG is the predominant form of POAG.[12–16]

People vary individually in the degree of excess ON length, which we term "redundancy," in central gaze. However, once the geometric inevitability of progressive adduction has consumed all redundancy by straightening the ON, a combination of two mechanical behaviors must occur to allow further adduction: ON elongation and globe translation. In normal people, the globe translates medially in adduction but does not retract.[3] Absence of globe retraction during adduction tethering in normal subjects suggests that that the normal ON may have sufficiently low stiffness (i.e. sufficient elasticity) to elongate in adduction under tensile force that is insufficient to retract the globe, thus applying low stress onto the ON head. The presence of globe retraction in patients with POAG, on the other hand, suggests a stiffer ON that does not elongate readily during adduction tethering, thus applying high stress onto the ON head. We therefore reason that ON elongation during adduction tethering represents an inverse indicator of stress on the ON head, and predict that this elongation will be subnormal in POAG where adduction tethering results in globe retraction. We also anticipated that a larger diameter globe would require, based on simple geometry of the movement of a point on a circular arc, that the globe-ON junction travel farther during rotation of a given angle then it would travel in a smaller eye.

We used high resolution MRI to quantify the change in ON path length during horizontal duction. A change in path length resulting from uncoiling a redundant, sinuous ON, however, does not represent a tensile strain that is readily interpretable by the foregoing scheme; the ON must be straight in the starting condition. Therefore, in order for change in ON length to represent actual tensile strain, we analyzed the changes in ON length from a position of adduction close to the threshold that removed redundancy from the ON compared with further

adduction beyond that position. While ON traction during adduction tethering includes vector components that tilt the optic disc and deform the peripapillary sclera, only the tensile force component coaxial with the ON induces elongation strain.

Methods

This research was approved prospectively by the Institutional Review Board for Protection of Human Subjects at University of California, Los Angeles, and adhered to tenets of the Declaration of Helsinki. Subjects were recruited for study of the biomechanical effects of eye movement and gave written informed consent prior to participation. The current study incorporates analysis of data obtained from normal subjects and patients with POAG whose IOP always measured below 21 mmHg without treatment. This constitutes additional analysis of data in most of these subjects who represent a subset of those included in a prior published report,[5] although one additional subject was studied following the prior publication. We did not exclude subjects who had been treated for IOP reduction with topical prostaglandin agonists, since nearly all patients with POAG are treated as first-line therapy with these drugs.[17–1819] We have shown that topical prostaglandin agonists do not alter anterior orbital fat in the regions exposed to these drugs[20] and multivariate analysis has not demonstrated a statistical effect of exposure to these drugs on globe retraction during adduction tethering.[5] We only selected for analysis all subjects who underwent target-controlled MRI in central gaze and smaller and larger angles of adduction who demonstrated minimal ON redundancy (path length <102.5% over minimum straight-line path) in both adduction positions. Analysis was also performed in two abduction angles, termed smaller and larger, corresponding to the same target positions as used to image the fellow orbits in adduction.

As described earlier,[5] high resolution orbital MRI was performed using a 1.5 T General Electric Signa scanner and dual-channel surface coil array (Medical Advances, Milwaukee, WI) using a T2-weighted, hydrogen nucleus, fast spin echo pulse sequence[21] with TR 3,700–4,000 ms, TE 80–85 ms, echo train length 13, pixel bandwidth 195 Hz, flip angle 90°, 100% phase field of view, row phase encoding direction, and two excitations. Quasi-coronal, 2-mm-thick images were obtained in contiguous sets of 17–20 planes perpendicular to the long axis of the orbit spanning from just anterior to the globe equator to the orbital apex (Figure 1a). The field of view was 8 × 8 cm and matrix 256x256, yielding 312 micron in-plane resolution. Typical quasi-coronal plane MRI acquisition time was about 2 minutes 40 seconds for each orbit per gaze position, varying modestly with subject weight.

Separate MRI acquisitions, in both axial and quasi-coronal (perpendicular to the long orbital axis) planes, were performed in each of five gaze positions for each eye. Eye position was controlled by monocular fixation of a small fiber optic target presented centrally and in ~25° and ~31° abduction. Since the adducting eye was unavoidably occluded by the surface coil or patient's nose, the fixating eye was imaged to obtain central and abduction positions, while the fellow eye was imaged to obtain adduction positions. Duction angles were determined from axial images, from the angle of a line passing through the cornea apex through the lens center and the estimated location of the fovea in the image best centered on the lens and optic nerve. This approach does not by itself account for the physiologic angle kappa, the angle between the subjective visual direction and the line of anatomic symmetry of the eye, that creates the appearance that the eye is slightly abducted even during straight-ahead viewing. The reported angle kappa averaged ~3°–5,°[22,23] similar to the angles measured here. Therefore, as done previously, the measured angle kappa in central gaze for each subject group was used to offset all measured angles for that group to achieve zero horizontal duction in central gaze.[5]

The most anterior image plane that included both ON and globe was defined as containing the globe-ON junction; this designation is slightly anterior to the criterion employed in our prior studies that did not aim to measure changes in ON length. The five image planes immediately posterior to the globe-ON junction were chosen for analysis because this portion typically featured well-defined demarcations between the ON and surrounding subarachnoid space (SAS) and sheath (Figure 1b), and avoided the transitional region between the anterior ON, lamina cribrosa, and optic disc. Using *ImageJ 64* software (http://imagej.nih.gov/ij/; provided in the public domain by the National Institutes of Health, Bethesda, MD, USA), the ON and inner border of the ON sheath were manually outlined. The cross-sectional areas and area centroids of those structures were then measured using *ImageJ 64* functions. The remaining analysis was automatically performed using custom algorithms written in *Excel* (Microsoft, Redmond, WA).

Three-dimensional Cartesian distances between ON area centroids in adjacent image planes were summed to calculate ON path length, while the angular differences between area centroids were used to geometrically correct cross-sectional area measurements for obliquity relative to MRI image planes using techniques described elsewhere.[24] Because ON cross-sectional areas typically decrease from anterior to posterior,[25] the ON cross-sectional areas of adjacent image slices were averaged to compute an interslice ON cross-sectional area for that image pair. Changes in ON interslice cross-sectional areas were compared between gaze positions to determine elongation or compression of that section of the ON.

The ON elongation calculation relied upon dual assumptions of uniform ON shape and conservation of ON volume between gaze positions (incompressibility with 0.5 Poisson ratio)[26] but did not require a circular ON cross-section because the volume in an image plane is the product of cross sectional area and plane thickness regardless of the shape of the cross section. Using those assumptions, change in ON length for each interslice pair was directly proportional to the change in interslice cross-sectional area between gaze positions, independent of the shape of the ON cross-section, equaling initial ON cross-sectional area minus final ON cross-sectional area, multiplied by initial ON interslice length. This calculation was performed for all four interslice regions and the differences in ON lengths summed to compute total ON elongation in the analysis region due to that gaze change.

Subarachnoid space (SAS) volume for each interslice segment was calculated by subtracting the ON cross-sectional areas from the areas bounded by the inner border of the ON sheath. As for the ON, the SAS cross-sectional areas in adjacent image slices were averaged and multiplied by computed ON length between those two image slices, corrected for path obliquity, to calculate the SAS partial volume (PV) for that segment of ON; this assumes that ON and ON sheath lengths correspond within each interslice segment. The differences in SAS PV between initial and final gaze positions were summed for all four interslice regions to compute total SAS PV change corresponding to that gaze change.

Changes in ON length and SAS PV were calculated for the gaze change from central gaze to smaller adduction and abduction; from smaller adduction and abduction to larger adduction and abduction; and finally, from central gaze to larger adduction and abduction. Globe displacement was determined by the shift of its centroid from central gaze to smaller and larger adduction and abduction relative to the orbit centroid.[5]

For statistical analysis, unpaired *t*-tests were performed using GraphPad Prism treating each eye as the unit of sampling. For the primary outcome of ON elongation, confirmatory analysis was repeated using the generalized estimating equation (GEE) method in SPSS software (IBM Corporation) that corrects for possible confounding by interocular correlations between eyes of individual subjects and has type 1 error characteristics superior to Student *t*-testing.[27] A variety of GEE multivariate models were evaluated to explore possible effects on ON elongation: diagnosis, age, gender, race, horizontal globe diameter, and axial globe length (AL). Finally, where GEE demonstrated significant effects, we explored these by simple linear regression using GraphPad Prism.

Results

Selection of eligible participants

It was first necessary to select for participation those subjects whose ONs were straight in both adduction position images; straightness was defined as less than 102.5% ON path redundancy. Of 34 orbits of patients with POAG without abnormally elevated IOP who had been imaged in smaller adduction, 26 (76%) has straight ONs in this gaze position and were selected for inclusion here. Of the remaining 8 orbits of patients with POAG that were not included, three demonstrated straight ONs in larger adduction. Overall 85% of patients with POAG thus met the path redundancy criterion for straightness for the larger adduction. Of 54 orbits of normal subjects who had been imaged in smaller adduction, 43 (80%) has straight ONs in this gaze position and were selected for inclusion as the control group. This fraction does not differ significantly from that of the patients with POAG (chi-square $P = .9$). Of the remaining 11 orbits of controls that were not included, 7 had straight ONs in larger adduction. Overall 92% of controls thus met the path redundancy criterion for straightness for the larger adduction. This fraction does not differ significantly from that of the patients with POAG (chi-square $P = .8$). It was therefore tentatively concluded that selection of subjects on the basis of ON straightness in small adduction was unlikely to introduce a confounding bias.

Characteristics of subjects included

The analysis thus included 38 orbits of 21 normal subjects (6 male, 15 female) and 22 orbits of 12 subjects with POAG without abnormally elevated IOP (5 male, 7 female). Two control subjects were Asian, 14 Caucasian, and five Black. Four subjects with POAG were Asian, 7 Caucasian, and one Black. Subjects with POAG were similar in age at 61 ± 11 yrs. (standard deviation) to controls at 53 ± 18 yrs. ($P = .17$), but had significantly larger horizontal globe diameters averaging 26.0 ± 0.9 mm versus 25.3 ± 1.0 mm ($P = .002$). We did not consider optical refraction data since most of the subjects had previously undergone cataract surgery, and their current refractive state had been artificially determined by intraocular lens selection. Axial length data from MRI were available for both eyes of all control subjects except for four, and averaged 24.3 ± 1.3 mm. Axial length data were available for both eyes of all subjects with POAG, and at an average of 25.3 ± 1.3 mm, was 1.0 mm significantly longer than controls ($P = .003$); the possible effect of this difference is explored below using multivariate analysis. The average perimetric mean deviation (MD) for the subjects with POAG in whom perimetry was available and interpretable was −6.1 ± 5.9 dB using the Humphrey Field Analyzer's 30–2 or 24–2 programs. Visual field loss in three eyes was too great to perform automated perimetry, so the preceding average value represents an underestimate. Based on inability to perform perimetry or MD,[28] 9 eyes were classified with severe, five moderate, and 8 mild VF loss, or were fellows of eyes with significant loss. Mean (±SD) minimum IOP was 8.8 ± 1.5 mmHg (±SD). Mean maximum IOP was 13.6 ± 4.0 mmHg. Mean central corneal thickness was 530 ± 33 microns. All except one eye of subjects with POAG were under treatment with topical prostaglandin agonist medications, as is clinically standard.

Duction Angles Achieved are illustrated in Figure 2. Reflecting consistency of target placement, the adduction angles achieved during MRI were similar between groups for both the smaller and larger angles at 23.7 ± 5.0°vs 24.9 ± 7.5°, and 29.6 ± 4.1° vs 31.4 ± 5.1° ($P > .17$) in subjects with POAG and controls, respectively. The abduction angles achieved during MRI were also similar between groups for both the smaller and larger angles at 22.7 ± 6.6° vs 23.4 ± 4.2°, and 29.4 ± 6.0° vs 28.6 ± 4.5° ($P > .5$) in subjects with POAG and normal subjects, respectively.

ON redundancy and straightness

The ON had significantly less redundancy in central gaze for normal subjects (102.5 ± 1.3% of minimum path length) than subjects with POAG (103.8 ± 1.7%, $P = .004$), but were almost identically straight in both smaller (101.4 ± 0.5% vs 101.6 ± 0.4%, $P = .14$) and larger (101.4 ± 0.5% vs 101.7 ± 0.5%, $P = .03$) adduction, respectively. The greater sinuosity of subjects with POAG was exaggerated by two outliers with extremely redundant ONs, but remained significant even with these excluded ($P = .012$). In both small and large abduction, the ON of subjects with POAG was also significantly more redundant than normal ($P < .0005$, Figure 3).

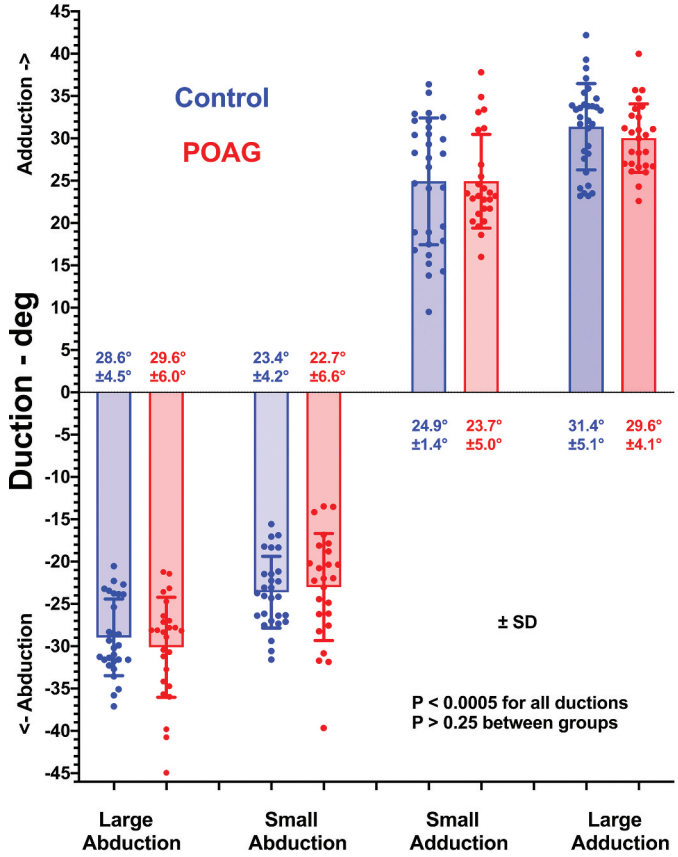

Figure 2. Mean duction angles achieved during MRI in control subjects, and subjects with primary open angle glaucoma (POAG). Dots represent individual measurements. Angles are corrected for angle kappa so that initial position is nominally zero. Values noted on columns differ significantly for each nominal gaze position in both groups, but not between groups for any nominal gaze position. SD – standard deviation.

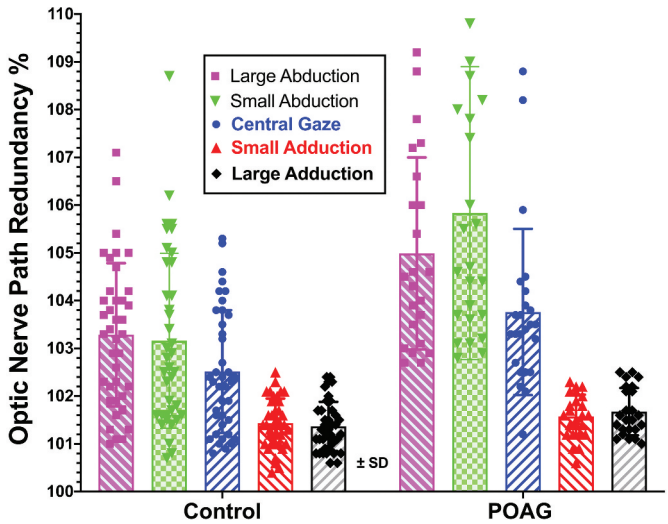

Figure 3. Actual optic nerve (ON) path length as a percentage of minimum distance from orbital apex to the globe for control subjects and subjects with primary open angle glaucoma (POAG). Dots represent individual measurements. Path redundancy was similarly minimal for small and large adduction for both groups, confirming that the ON was straight in both adduction angles. However, ON path in POAG was significantly more redundant than normal in central gaze and abduction ($P < .005$) SD – standard deviation.

Optic nerve volume and elongation

As expected because POAG is an atrophic optic neuropathy, in central gaze the mean ON PV of 61 ± 12 mm^3 PV in subjects with POAG was significantly less than that of the healthy control group at 67 ± 8 mm^3 ($P = .02$). Elongation of the ON in the anterior region spanned by contiguous MRI planes beginning at the globe-ON junction was computed by summing local elongations computed for the four pairs of adjacent planes in the region. As evident for examination of each of the four pairs analyzed for the gaze change from central to large adduction graphed in Figure 4, the average normal ON elongated in each pair in large adduction, while in subjects with

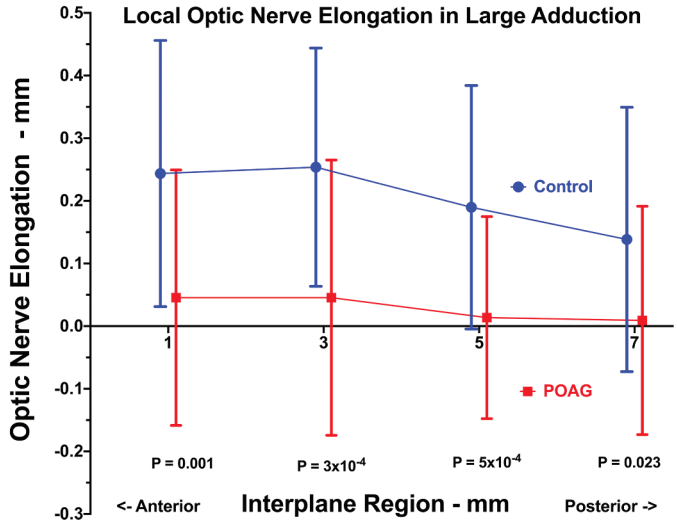

Figure 4. Mean optic nerve elongation from central gaze to large adduction in each adjacent 2 mm thick interslice analysis segment. Control subjects demonstrated significant elongation, while subjects with primary open angle glaucoma (POAG) did not. Error bars represent standard deviation. Abscissa values are offset slightly to avoid overlap.

POAG the ON did not. The elongation was slightly greater anteriorly than posteriorly in normal subjects (Figure 4). In the interest of clarity, however, in the remainder of this report we consider only the summed ON elongation in all four MRI plane pairs, as summarized in Figure 5 and to which we now refer for brevity as "ON elongation." In subjects with POAG, there was no significant ON elongation in large or small adduction or abduction (Figure 5). While this was also the case for normal subjects in abduction, there was highly significant ON elongation averaging 0.44 ± 0.49 mm in small ($P < 10^{-7}$) and 0.81 ± 0.56 mm in large adduction ($P < 10^{-18}$, by two-tail *t*-testing vs. zero). The incremental adduction from small to large corresponded to ON elongation of 0.39 ± 0.47 mm in controls compared with no significant change in ON length (0.15 ± 0.38 mm) in POAG ($P > .03$). The difference in elongation in adduction was highly significantly greater in control subjects than in POAG ($P < 10^{-.5}$).

Subarachnoid space volume

Mean SAS PV in central gaze was about 43 mm^3 and did not differ significantly between groups (Figure 6). In the control group, mean SAS PV decreased significantly from 42 ± 18 mm^3 to 31 ± 16 mm^3 ($P = .007$) from central gaze to smaller adduction and did not change significantly from smaller adduction to larger adduction where it averaged 33 ± 16 mm^3. For subjects with POAG, mean SAS PV decreased insignificantly from 44 ± 27 mm^3 to 37 ± 27 mm^3 ($P = .34$) from central gaze to

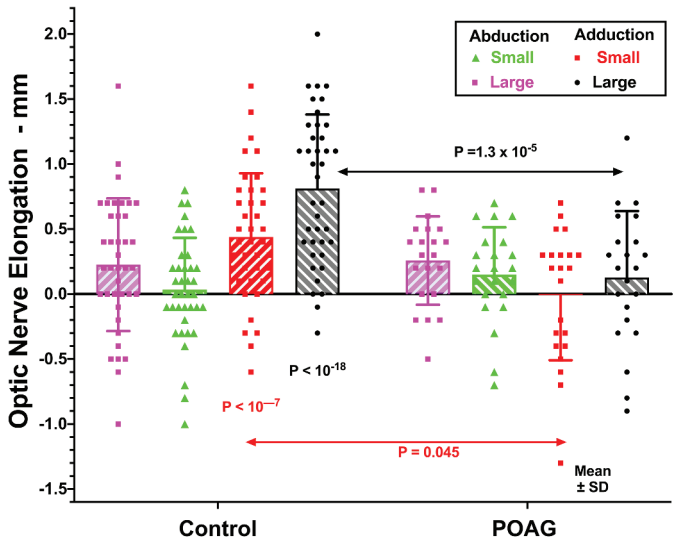

Figure 5. Optic nerve elongation during gaze shifts from central to small and large abduction and adduction in control subjects and in primary open angle glaucoma (POAG). Symbols represent data for individual orbits. ON elongation for POAG was not significantly different from zero, but was highly significantly so for adduction but not abduction in controls. SD – standard deviation.

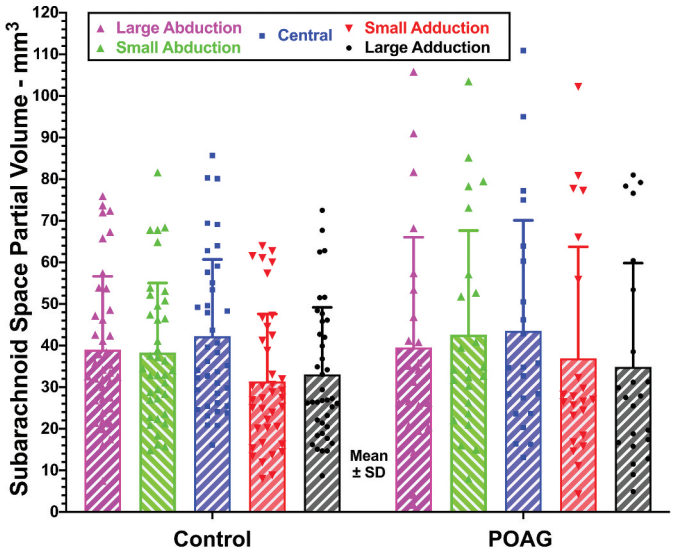

Figure 6. Subarachnoid space volume was quantitatively similar in control subjects and subjects with primary open angle glaucoma (POAG), and decreased similarly from central gaze to small adduction, but did not further decrease with larger adduction. In both groups, there was a smaller decrease in large abduction. SD – standard deviation.

smaller adduction and did not change significantly from smaller adduction to 35 ± 25 mm^3 in larger adduction. Thus, the gaze shift from central to large adduction was associated with 9 μL decrease in SAS volume in both subject groups.

During abduction, SAS PV also decreased, but only about half as much as during adduction. For the control group, total SAS PV decreased by 5 ± 14 mm^3 from central gaze to smaller abduction, and then increased by an insignificant 2 ± 10 mm^3 from smaller to large abduction. For subjects with POAG, SAS PV did not change (0.5 ± 10 mm^3, P = .19 vs controls) from central gaze to smaller abduction, and decreased by 5 ± 9 mm^3 from smaller to larger abduction (P = .01 vs controls). From central gaze to large abduction, SAS PV decreased similarly in the two groups by 3 ± 12 mm^3 for controls and 5 ± 12 mm^3 for POAG (P = .51).

Globe translation

As illustrated in Figure 7a, in small adduction, control subjects exhibited 0.2 ± 0.6 mm posterior globe translation, similar to subjects with POAG at 0.4 ± 0.9 mm (P = .25). In large adduction, control subjects exhibited no further posterior globe translation that remained 0.2 ± 0.5 mm, while subjects with POAG demonstrated significantly more globe retraction at 0.6 ± 0.7 mm (P = .027). Likewise, Figure 7b illustrates that both control and subjects with POAG demonstrated similar medial globe shifts with both smaller adduction (0.8 ± 0.6 mm for controls and 0.7 ± 0.5 mm for subjects with POAG, P = .65) and larger adduction (0.8 ± 0.5 mm for controls, 0.6 ± 0.5 mm for subjects with POAG (P = .10).

Multivariate Analysis of Optic Nerve Elongation in adduction was performed using GEE, considering as factors the presence of POAG, race, and gender, as well as the intra-subject variable of each eye. Subject age, horizontal globe diameter, and AL were considered as covariates. These models accounted for possible inter-eye correlations in subjects who contributed data on both eyes. Subject age, race, gender, and horizontal globe diameter showed no significant effect (P > .4) on elongation of the ON for smaller or larger adduction. However, in multivariate models the presence of POAG had a highly significant effect on elongation of the ON in both smaller and larger adduction (P = .0002). Axial length had a significant effect of increasing elongation of the ON for smaller adduction (P = .012), but only a borderline effect for larger adduction (P = .051). For larger adduction and considering only cases where AL was available, the effect on elongation of the ON of POAG remained significant at P = .0002, and of AL at P = .015.

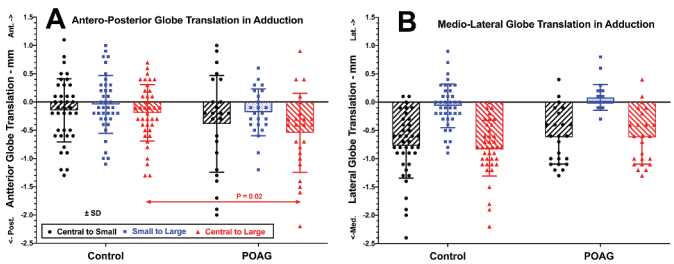

Figure 7. Globe translation during horizontal duction. a. Posterior globe translation in adduction was greater in POAG than in controls. b. Medial globe translation in adduction was similar in POAG and controls.

Regression analysis of optic nerve elongation

The effect of AL on elongation of the ON in larger adduction was then examined by simple linear regression (Figure 8). Based on regression slopes, for each mm increase in AL, ON elongation increased by 0.16 ± 0.08 mm in controls and by 0.19 ± 0.07 mm in subjects with POAG (± standard error). These values did not differ significantly from one another, but were significantly different from zero ($P < .05$), implying that increasing AL similarly increases ON elongation in controls and subjects with POAG. However, the coefficients of determination (R^2) indicate that AL accounts for only about 14% of the variation in ON elongation in controls, and 30% in subjects with POAG.

A similar analysis was performed for the change in SAS volume between central gaze and larger adduction. This showed no significant effect of AL in either subject group ($P > .1$). This finding for the SAS is again interpreted as evidence that changes based on cross section due to adduction are specific to the ON itself, rather than to the technique or tissues in its vicinity.

Discussion

During adduction tethering, the ONs of healthy subjects elongated significantly with little globe retraction, while those of subjects with POAG at normal IOP who had mild to severe visual field loss on average did not elongate significantly while the globe retracted significantly more. This implies that the straight ONs of healthy subjects stretch to exceed their straight, unloaded lengths during adduction tethering, while the straight ONs of subjects with POAG stretched little or none on despite being tethered. The study thus confirmed the prediction of abnormally high ON stiffness in POAG at normal IOP. More subtly, the present data suggest that ON elongation during adduction tethering increases with increasing AL, both in healthy subjects and in subjects with POAG at normal IOP (Figure 8). This latter finding is consistent with geometry of the globe and orbit, which requires that the globe-ON junction travel farther in larger than smaller diameter eyes, with consequent greater increase in ON path length during adduction tethering. While a few highly myopic subjects with POAG did exhibit some ON elongation during adduction tethering (Figure 8), elongation was so much less or even negative in most of them that the overall average remained close to zero. Thus, the ON was also stiff in the more highly myopic subjects with POAG.

Volume of the SAS in the region 8 mm posterior to the globe decreased similarly by 9 mm^3 during adduction tethering in both groups, presumably reflecting cerebrospinal fluid redistribution during the eye movement, but in particular providing an internal control for this study demonstrating specificity of PV changes related to elongation of the ON itself, rather than merely to general changes within the ON sheath or different fluid fluxes in the ON itself. This change in PV with gaze shift is significant, amounting to as much as almost 25% of total SAS volume in the immediate retrobulbar region. The ON shift within the SAS might function as a local pumping mechanism for cerebrospinal fluid driven by horizontal eye movements, providing some bulk flow to and from the 8 mm retrobulbar ON segment. Even if CSF fluid flow were entirely oscillatory, this phenomenon could serve as an agitator to circulate nutrients, analogous to the facilitation of ocular perfusion driven by oscillatory saccadic eye rotations in birds.[29]

The approximately 30° adductions employed in this study were only a little more than half of the roughly 55° oculomotor range.[30] Much larger conjugate horizontal eye movements are quite normal, and around three of them occur each second,[31] adding up to about 183,000 daily.[32] Saccades are unceasing even while we are asleep.[33] The largest saccades do not occur during laboratory or clinical settings, but rather in active daily life during voluntary head movements[34] and ambulation. When head and body are both unrestrained, 25–45°saccades frequently occur,[34] including unconscious ocular counter-rotations generated by the vestibulo-ocular reflex.[35] Horizontal saccades of over 40° occur during

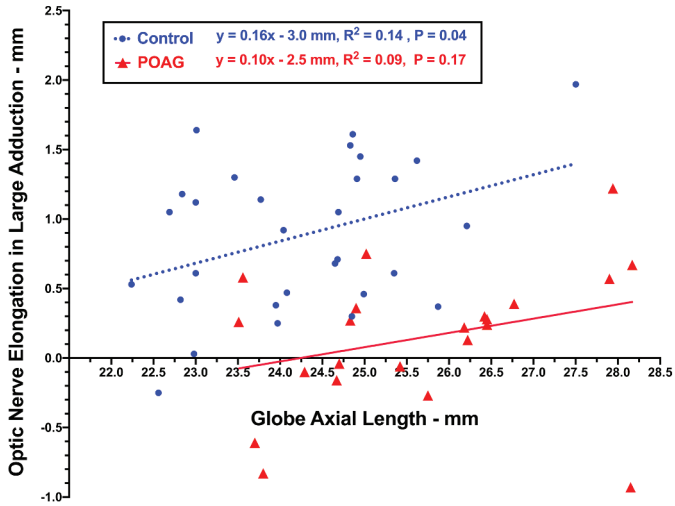

Figure 8. Linear regressions demonstrate effects of globe axial length (AL) on optic nerve elongation in large adduction. Regression slopes were significantly non-zero but did not differ between groups, showing a significant effect of AL ($P < .05$).

everyday tasks such as walking, ball catching, visual search, and tea making.[36] Of course, small eye movements during reading probably do not create enough adduction to tether the ON. Although the reader may be tempted to think that convergence may induce adduction retraction, this is not the case. Not only is maximal physiological convergence insufficient to achieve adduction tethering with a centered near target, the geometrically required convergence angle for laterally eccentric targets is less than for a centered target.[37] Even convergence of 22°, which is only briefly sustainable with great effort, is associated with globe proptosis rather than retraction.[38]

The current study, therefore, utilized a modest and physiological degree of adduction likely to occur often in daily life. About 80% of orbits imaged, both controls and patients with POAG, exhibited ON straightening when adduction reached 25°, and about 90% of both groups did so when adduction increased further to about 31°. In healthy people, after actual ON path increases to exhaust the ON's relaxed length, the ~6° additional adduction elongated the average ON by around 10%. This elongation dissipates ON stress caused by reaction to MR contractile force and thus averts globe retraction. The present finding at least in part explains that in POAG, failure of the pathologically stiffer ON to stretch in the normal manner under adduction stress transfers the force of MR contraction onto the globe to retract it. Moreover, this failure of ON stretching in POAG is likely to create more of these effects in people whose shorter ONs predispose to tethering at lesser adduction, and thus more globe retraction when larger adduction occurs.

Assuming in POAG that the intrinsic mechanical properties of non-sinuous ONs are typical of sinuous ones, the difference in ON elasticity would explain a seemingly paradoxical observation regarding the role of adduction-induced ON strain in POAG: the abnormally greater average ON path redundancy in central gaze.[3–5] A more redundant ON path in central gaze might have been expected to create less traction on the globe during adduction, yet the globe retraction in adduction observed in POAG suggests abnormally greater traction.[3–5] This seeming paradox may be resolved by considering the difference in mechanical behaviors between a rubber band and an inelastic string. A rubber band stretches and relaxes with increasing and decreasing strain, maintaining a relatively uniform, straight path between two suspensory points as long as the distance between the points exceeds the rubber band's relaxed length. Conversely, an inelastic string sags with little force on two suspensory points until progressive extension has removed all slack, but then becomes stiffly taut to firmly resist further elongation. The healthy ON behaves like a compliant rubber band, maintaining a path between orbital apex and globe that is only mildly redundant in central gaze but not redundant in adduction, while the ON in NTG behaves like an inelastic string, sagging more redundantly in central gaze yet becoming stiffly taut in larger adduction where it retracts the globe. In larger adduction, for example, a similar proportion of controls and patients with POAG exhibited ON tethering despite these differences in ON length in central gaze.

Computational biomechanical modeling using finite element analysis (FEA) demonstrates that adduction-induced mechanical strain applied to the globe is distributed in the same region as the temporal peripapillary atrophy typically found in patients with POAG at normal IOP.[39,40] It is suggested by FEA that adduction-induced mechanical strain on the lamina cribrosa could markedly exceed the strain created by an IOP of 45 mmHg, which has been observed to be small both *in vivo*[41] and *ex vivo*.[42] Simulation also suggests that the peripapillary and lamina cribrosa strain created by adduction tethering is exaggerated when the ON is stiffer (Park and Demer, unpublished data 2020). Thus, adduction-induced mechanical strain might play a causative role in the development of ON atrophy.[40]

The etiology of this pathological ON stiffening in POAG is unclear. Perhaps the intrinsic connective tissue structure within of the ON is different in POAG with normal IOP, either as a cause of susceptibility to the disease itself or through pathologic remodeling as a result of the disease. Both of these mechanisms might be operative if, for example ON stiffening in the face of repetitive adduction tethering causes axonal damage that in turn induces further ON stiffening through tissue remodeling, in a deleterious feedback loop. The ON itself contains an extensive connective structure encompassing a substantial fraction of its total cross sectional area and in intimate relationship to the thick ON pia mater,[25] accounting for the high mechanical stiffness of the ON[39] and its sheath.[43] Regardless of etiology, the larger than normal AL in subjects with POAG moves the globe-ON junction farther laterally during adduction, increasing the strain applied onto the globe during ON tethering. The association between globe size and increased adduction-induced strain on the disc and peripapillary region may contribute to the higher prevalence of glaucoma in myopia, where AL is typically enlarged.[44]

A reformatted x-ray tomographic study reported in patients with POAG at normal IOP that the external diameter of the retrobulbar ON sheath is 1 mm larger than controls in the region 3 mm posterior to the globe-ON junction.[45] This study did not control for gaze position, could not separately resolve the ON from the SAS or sheath, did not use cross-sectional area, and included controls suspected of stroke. Given the 20–25% reduction in SAS volume observed here during adduction in both POAG and normal controls, we caution that any imaging protocol designed to provide quantitative measurements of the SAS can be substantially erroneous unless gaze position is controlled.

The current study is limited by small sample sizes and by differences in average globe size between study groups, yet small sample size would tend to work against the demonstration of significant intergroup differences that were found, not create false differences or exaggerate significance of differences. An important consideration may be an inherent difference in ON redundancy related to existence of POAG, insofar as in central gaze the healthy control group had significantly less ON redundancy than the subjects with POAG. Since normal ON paths were already nearly straight prior to even smaller adduction, more tethering should be applied to the typical normal than POAG globe for a given adduction angle, even with the smaller average globe diameter. This lack of ON redundancy likely accounted for the 0.4 mm ON elongation measured in healthy controls adducting from central gaze to 25°; it is probable that at least some healthy people develop ON tethering at angles even less than 25°. The normal ON elongated another 0.4 mm when adduction continued from 25° to 31°, however, demonstrating that additional adduction beyond the point where the ON tethered the globe created significant additional strain. The absence of either significant ON elongation or globe

retraction in the subjects with POAG at smaller adduction angles, on the other hand, supports the inference that greater ON redundancy in central gaze prevents strain against the globe until larger adduction angles are reached. Such large eye movements are common in daily life.[3,5,7] Once the limit in ON redundancy has been exhausted by larger adduction angles, the pathologic ON nerve tethers and retracts the globe with subnormal stretching. The reason for the longer than normal ON in POAG is currently enigmatic.

These overall findings provide evidence that the ON is abnormally stiff in people with mild to severe visual field loss due to POAG at normal IOP. Rather than normally elongating to dissipate MR reaction force during adduction tethering, in POAG the stiff ON resists elongation so much that the globe must retract. The resulting transfer of mechanical strain to the disc and peripapillary region of the globe provides further support to the notion that adduction tethering is one of perhaps multiple plausible etiologies for progressive ON atrophy in POAG without abnormally elevated IOP.

Acknowledgments

This work was supported by the US Public Health Service, Washington, DC, under NEI Grants EY008313 and EY00331, and by an unrestricted grant to the Department of Ophthalmology from Research to Prevent Blindness, New York, NY. The funding organizations had no role in the design or conduct of this research.

Disclosure statement

None of the authors has a financial interest in any material related to this paper.

Funding

This work was supported by the US Public Health Service, Washington, DC, under NEI Grants [EY008313 and EY000331] and by an unrestricted grant from Research to Prevent Blindness, New York, NY. The funding organizations had no role in the design or conduct of this research.

ORCID

Robert A. Clark http://orcid.org/0000-0002-2422-0337

References

1. Lockwood CB. The anatomy of the muscles, ligaments, and fasciae, etc. J Anat Physiol. 1886;20:1–25.
2. Suh SY, Clark RA, Demer JL. Optic nerve sheath tethering in adduction occurs in esotropia and hypertropia, but not in exotropia. Invest Ophthalmol Vis Sci. 2018;59(7):2899–904. doi:10.1167/iovs.18-24305.
3. Demer JL, Clark RA, Suh SY, Giaconi JA, Nouri-Mahdavi K, Law SK, Bonelli L, Coleman AL, Caprioli J. Magnetic resonance imaging of optic nerve traction during adduction in primary open-angle glaucoma with normal intraocular pressure. Invest Ophthalmol Vis Sci. 2017;58(10):4114–25. doi:10.1167/iovs.17-22093.
4. Demer JL. Optic nerve sheath as a novel mechanical load on the globe in ocular duction. Invest Ophthalmol Vis Sci. 2016;57(4):1826–38. doi:10.1167/iovs.15-18718.
5. Demer JL, Clark RA, Suh SY, Giaconi JA, Nouri-Mahdavi K, Law SK, Bonelli L, Coleman AL, Caprioli J. Optic nerve traction during adduction in open angle glaucoma with normal versus elevated intraocular pressure. Curr Eye Res. 2019;45(2):199–210. doi:10.1080/02713683.2019.1660371.
6. Clark RA, Isenberg SJ. The range of ocular movements decrease with aging. J Aapos. 2001;5(1):26–30. doi:10.1067/mpa.2001.111016.
7. Chang MY, Shin A, Park J, Nagiel A, Lalane RA, Schwartz SD. Deformation of the optic nerve head and peripapillary tissue by horizontal duction. Am J Ophthalmol. 2017;174:85–94. doi:10.1016/j.ajo.2016.10.001.
8. Le A, Chen J, Lesgart M, Gawargious BA, Suh SY, Demer JL. Age-dependent deformation of the optic nerve head and peripapilary retina by horizontal duction. Am J Ophthalmol. 2020;209:107–16. doi:10.1016/j.ajo.2019.08.017.
9. Suh SY, Le A, Shin A, Park J, Demer JL. Progressive deformation of the optic nerve head and peripapillary structures by graded horizontal duction. Invest Ophthalmol Vis Sci. 2017;58(12):5015–21. doi:10.1167/iovs.17-22596.
10. Demer JL, Clark RA. Translation and eccentric rotation in ocular motor modeling. Prog Brain Res. 2019;248:117–126.
11. Clark RA, Demer JL. The effect of axial length on extraocular muscle leverage. Am J Ophthalmol. 2020;216:186–92. doi:10.1016/j.ajo.2020.03.033.
12. Shi D, Funayama T, Mashima Y, Takano Y, Shimizu A, Yamamoto K, Mengkegale M, Miyazawa A, Yasuda N, Fukuchi T, et al. Association of hk2 and nck2 with normal tension glaucoma in the Japanese population. PloS One. 2013;8(1):e54115. doi:10.1371/journal.pone.0054115.
13. Iwase A, Suzuki Y, Araie M, Yamamoto T, Abe H, Shirato S, Kuwayama Y, Mishima HK, Shimizu H, Tomita G, et al. The prevalence of primary open-angle glaucoma in Japanese: the Tajimi study. Ophthalmology. 2004;111(9):1641–48. doi:10.1016/j.ophtha.2004.03.029.
14. Kim CS, Seong GJ, Lee NH, Song KC, NSG KGS. Prevalence of primary open-angle glaucoma in central South Korea: the Namil study. Ophthalmology. 2011;2011:1024–30. doi:10.1016/j.ophtha.2010.10.016.
15. Ha A, Kim YK, Jeoumg JW, Kim DM, Park KH. Association of angle width with progression of normal-tension glaucoma: a minimum 7-year follow-up study. JAMA Ophthalmol. 2019;137(1):13–20. doi:10.1001/jamaophthalmol.2018.4333.
16. Zhao J, Solano MM, Oldenburg CE, Liu T, Wang Y, Wang N, Lin SC. Prevalence of normal-tension glaucoma in the chinese population: a systematic review and meta-analysis. Am J Ophthalmol. 2019;199:101–10. doi:10.1016/j.ajo.2018.10.017.
17. Li T, Lindsley K, Rouse B, Hong H, Shi Q, Friedman DS, Wormald R, Dickersin K. Comparative effectivenss of first-line medications for primary open-angle glaucoma: a systematic review and network meta-analysis. Ophthalmology. 2016;123(1):129–40. doi:10.1016/j.ophtha.2015.09.005.
18. Wang K, Zu L, Yuan Z, Yao K, Zhao J, Zu L, Fang A, Zhang M, Wu L, Ji J. Intraocular pressure-lowering efficacy and safety of bimatoprost 0.03% therapy for primary open-angle glaucoma and ocular hypertension patients in China. BMC Ophthalmol. 2014;14(1):21. doi:10.1186/1471-2415-14-21.
19. Winkler NS, Fautsch MP. Effects of prostaglandin analogues on aqueous humor outflow pathways. J Ocul Pharmacol Ther. 2014;30(2–3):102–09. doi:10.1089/jop.2013.0179.
20. Chen J, Le A, Caprioli J, Giaconi JA, Nouri-Mahdavi K, Law SK, Bonelli L, Coleman AL, Demer JL. Orbital fat volume after treatment with topical prostaglandin agonists. Invest Ophthalmol Vis Sci. 2020;61(5):46. doi:10.1167/iovs.61.5.46.
21. Demer JL, Dushyanth A. T2-weighted fast spin-echo magnetic resonance imaging of extraocular muscles. J Aapos. 2011;15(1):17–23. doi:10.1016/j.jaapos.2010.12.006.
22. Basmak H, Sahin A, Yildirim N, Saricicek T, Yurdakul S. The angle kappa in strabismic individuals. Strabismus. 2007;15(4):193–96. doi:10.1080/09273970701631926.
23. Gharaee H, Shafiee M, Hoseini R, Abrishami M, Abrishami Y, Abrishami M. Angle kappa measurements: normal values in healthy Iranian population obtained with Orbscan II. Iran Red Crescent Med J. 2015;17:e17873. doi:10.5812/ircmj.23191v2.
24. Clark RA, Demer JL. Functional morphometry of horizontal rectus extraocular muscles during ocular duction. Invest Ophthalmol Vis Sci. 2012;53:7375–79. doi:10.1167/iovs.12-9730.

25. Karim S, Clark RA, Demer JL. Demonstration of systematic variation in human intraorbital optic nerve size by quantitative magnetic resonance imaging and histology. Invest Ophthalmol Vis Sci. 2004;45:1026–33. doi:10.1167/iovs.03-1246.
26. Kim H, Yoo L, Shin A, Demer JL. Determination of Poisson ratio of bovine extraocular muscle by computed x-ray tomography. BioMed Res Int. 2013;2013:1–5. Article ID 197479. doi:10.1155/2013/197479.
27. Huang J, Huang J, Chen Y, Ying G. Evaluation of approaches to analyzing continuous correlated eye data when sample size is small. Ophthalmic Epidemiol. 2018;25(1):45–54. doi:10.1080/09286586.2017.1339809.
28. Forchheimer I, de Moraes CG, Teng CC, Folgar F, Tello C, Ritch R, Liebmann JM. Baseline mean deviation and rates of visual field change in treated glaucoma patients. Eye. 2011;25(5):626–32. doi:10.1038/eye.2011.33.
29. Pettigrew JD, Wallman J, Wildsoet CF. Saccadic oscillations facilitate ocular perfusion from the avian pecten. Nature. 1990;343(6256):362–3
30. Guitton D, Volle M. Gaze control in humans: eye-head coordination during orienting movements to targets within and beyond the oculomotor range. J Neurophysiol. 1987;58(3):427–59. doi:10.1152/jn.1987.58.3.427.
31. Wu CC, Kowler E. Timing of saccadic eye movements during visual search for multiple targets. J Vision. 2013;13(11):1–21. doi:10.1167/13.11.11.
32. Robinson DA. Control of eye movements. In: Brooks VB, editor. The nervous system, handbook of physiology. Baltimore (MD): Williams & Wilkins; 1981. p. 1275–320.
33. Leclair-Visonneau L, Oudiette D, Gaymard B, Leu-Semenescu S, Arnulf I. Do the eyes scan dream images during rapid eye movement sleep? Evidence from the rapid eye movement sleep behaviour disorder model. Brain. 2010;133:1737–46.
34. Anastasopoulos D, Ziavra N, Hollands M, Bronstein A. Gaze displacement and inter-segmental coordination during large whole body voluntary rotations. Exp Brain Res. 2009;193(3):323–36. doi:10.1007/s00221-008-1627-y.
35. Anastasopoulos D, Naushahi J, Sklavos S, Bronstein AM. Fast gaze reorientations by combined movements of the eye, head, trunk and lower extremities. Exp Brain Res. 2015;233(5):1639–50. doi:10.1007/s00221-015-4238-4.
36. Kothari R, Yang Z, Kanan C, Bailey R, Pelz JB, Diaz GJ. Gaze-in-wild: a dataset for studying eye and head coordination in everyday activities. Sci Rep. 2020;10(1):2539. doi:10.1038/s41598-020-59251-5.
37. Tian JR, Mokono E, Demer JL. The vestibulo-ocular reflex to transient surge translation: complex geometric response ablated by normal aging. J Neurophysiol. 2006;95(4):2042–54. doi:10.1152/jn.00635.2005.
38. Demer JL, Kono R, Wright W. Magnetic resonance imaging of human extraocular muscles in convergence. J Neurophysiol. 2003;90:2072–85. doi:10.1152/jn.00636.2002.
39. Shin A, Yoo L, Park C, Demer JL. Finite element biomechanics of optic nerve sheath traction in adduction. J Biomech Eng. 2017;139(10):101010. doi:10.1115/1.4037562.
40. Wang X, Fisher LK, Milea D, Jonas JB, Girard MJA. Predictions of optic nerve traction forces and peripapillary tissue stresses following horizontal eye movements. Invest Ophthalmol Vis Sci. 2017;58(4):2044–53. doi:10.1167/iovs.16-21319.
41. Wang YX, Jiang R, Wang NL, Xu L, Jonas JB. Acute peripapillary retinal pigment epithelium changes associated with acute intraocular pressure elevation. Ophthalmology. 2015;122(10):2022–28. doi:10.1016/j.ophtha.2015.06.005.
42. Midgett D, Liu B, Ling YTT, Jeffreys JL, Quigley HA, Nguyen TD. The effects of glaucoma on the pressure-induced strain response of the human lamina cribosa. Invest Ophthalmol Vis Sci. 2020;61:41. doi:10.1167/iovs.61.4.41.
43. Shin A, Park J, Le A, Poukens V, Demer JL. Bilaminar mechanics of the human optic nerve sheath. Curr Eye Res. 2019;17:1–10.
44. Shim SH, Sung KR, Kim JM, Kim HT, Jeong J, Kim CY, Lee MY, Park KH. The prevalence of open-angle glaucoma by age in myopia: the Korean national health and nutrition survey. Curr Eye Res. 2017;42(1):65–71.
45. Pircher A, Montali M, Berberat J, Remonda L, Killer HE. Relationship between the optic nerve sheath diameter and lumbar cerebrospinal fluid pressure in patients with normal tension glaucoma. Eye. 2017;31(9):1365–72. doi:10.1038/eye.2017.70.